

# Quantifying Crystal Form Content in Physical Mixtures of (±)-Tartaric Acid and (+)-Tartaric Acid Using Near Infrared Reflectance Spectroscopy

Submitted: February 1, 2005; Accepted: April 28, 2005; Published: October 6, 2005

Paul E. Luner<sup>1,2</sup> and Aditya D. Patel<sup>1,3</sup>

<sup>1</sup>Division of Pharmaceutics, College of Pharmacy, University of Iowa, Iowa City, Iowa 52242

<sup>2</sup>Current Address: Pfizer Inc, Global Research and Development, Groton Laboratories, Pharmaceutical Research and Development, Eastern Point Road 8156-102, Groton CT 06340

<sup>3</sup>Current Address: Helios Pharmaceuticals, 'Helios House' 659/1, Panchwati Ahmedabad-380015 Gujarat, India

## ABSTRACT

The objective of this study was to use diffuse reflectance near infrared spectroscopy (NIRS) to determine racemic compound content in physical mixtures composed primarily of the enantiomorph and to assess the error, instrument reproducibility and limits of detection (LOD) and quantification (LOQ) of the method. Physical mixtures ranging from 0 to 25% (±)-tartaric acid in (+)-tartaric acid were prepared and spectra of the powder samples contained in glass vials were obtained using a Foss NIRSystems Model 5000 monochromator equipped with a Rapid Content Analyzer scanning from 1100 to 2500 nm. A calibration curve was constructed by plotting (±)-tartaric acid weight percent against the 2<sup>nd</sup> derivative values of  $\log(1/R)$  vs  $\lambda$  at a single wavelength, normalized with a denominator wavelength (1480 nm/1280 nm). Excellent linearity was observed ( $R^2=0.9999$ ). The standard error of calibration (SEC) was 0.07 and the standard error of prediction (SEP) for the validation set was 0.11. Instrument and method errors for samples in the 2% composition range ((±)-tartaric acid in (+)-tartaric acid) were less than 1% RSD and 3% RSD, respectively. The practical LOD and LOQ were 0.1% and 0.5%, respectively, and comparable to the calculated LOD and LOQ. These studies show that NIRS can be used as a rapid and sensitive quantitative method for determining racemate content in the presence of the enantiomerically pure crystal in the solid-state.

**KEYWORDS:** Tartaric Acid, near-infrared spectroscopy, crystal form, quantification, enantiomers, racemate.

## INTRODUCTION

Enantiomers or racemates comprise of more than one half of the drugs that are sold worldwide.<sup>1</sup> Enantiomers exhibit differences in their pharmacological and toxicological

properties because they can interact with stereoselective biological macromolecules.<sup>2</sup> In the crystalline state, enantiomers and the corresponding racemic compound may differ considerably in their physicochemical properties. Crystallization from a racemic solution may result in formation of a racemate as a minor impurity and the racemate may be either a mixture of pure homochiral crystals (racemic conglomerate) or single racemic crystals (racemic compound).<sup>3</sup> Traces of enantiomeric impurity can cause a significant change in the physicochemical properties of crystals formed from a single enantiomer.<sup>4</sup> Solid-state processing such as milling, grinding or exposure to relative humidity are known to induce transformation of conglomerates to racemic compounds.<sup>5</sup>

Solid-state methods that are rapid and capable of differentiating the racemic compound from the pure enantiomer crystal form would be particularly useful for investigating solid-state physical and chemical stability issues and processing effects that have an impact on formulation of solid dosage forms.

FTIR spectroscopy<sup>6</sup> and XRPD<sup>7,8</sup> have been used to quantify the racemic compound in the pure enantiomer. However, both these methods can require particle size reduction of the samples by grinding, which may alter the physical state of the sample. Determination of enantiomeric composition in solvents can be accomplished using <sup>1</sup>H- or <sup>13</sup>C-NMR methods using chiral shift reagents.<sup>9,10</sup> The utility of solid-state <sup>13</sup>C NMR to distinguish optically pure from racemic crystals was shown by Hill et al.<sup>11</sup> DSC has also been applied to quantify enantiomers.<sup>12</sup> With the exception of FTIR, none of the aforementioned methods are typically as rapid or require as little sample preparation as Near Infrared Reflectance Spectroscopy (NIRS).

The feasibility of using NIRS for determination of enantiomeric purity was previously reported for *l*- and *dl*-valine using a multiple linear regression method.<sup>13</sup> However, quantitative limits and extent of errors were not investigated nor was an independent sample set employed for validation. The application of univariate near infrared reflectance spectroscopy methods for solid-state form

---

**Corresponding Author:** Paul E. Luner, Pfizer Inc., Global Research and Development, Groton Laboratories  
Pharmaceutical Research and Development, Eastern Point Road 8156-102, Groton CT 06340. Tel: (860)441-3628; Fax: (860)441-3972. Email: paul.e.luner@pfizer.com

quantification (amorphous content, polymorphs and hydrates) of APIs and excipients in binary mixtures has been demonstrated for small samples sets.<sup>14,15</sup> As a further extension of this approach, it was therefore of interest to more fully investigate NIRS for the determination of the racemic compound in the presence of the pure enantiomer using a study design suitable for small numbers of samples and limited calibration sets aimed at the formulation development level. Binary physical mixtures of crystalline ( $\pm$ )-tartaric acid (racemic compound) and (+)-tartaric acid (l-form) were used as a model system. Absolute error, standard error of prediction and limits of detection and quantification were evaluated. The differences in the NIR spectra were interpreted based on solid-state characterization data and crystal structures. The quantitative limits obtained in this study were also compared with results from other solid-state methods reported in the literature.

## MATERIALS AND METHODS

[(R,R), (S,S)]-2,3 dihydroxybutanedioic acid (DL-tartaric acid anhydrous; ( $\pm$ )-TA) and (R,R)-2,3 dihydroxybutanedioic acid (L-tartaric acid; (+)-TA) were obtained from Sigma Chemical Co (St. Louis, MO). Additional lots of ( $\pm$ )-TA and (+)-TA were obtained from Aldrich Chemical Co., Inc. (Milwaukee, WI) to study the robustness of the calibration models. Both materials were sieved using a sonic sifter (Allen-Bradley, Milwaukee, WI) to obtain a size fraction of 38 to 150  $\mu\text{m}$ . To achieve the desired particle size for (+)-TA, it was first ground in a mortar and pestle.

### NIRS Quantitative Studies

#### NIRS Sample Preparation

Physical mixtures of the ( $\pm$ )-TA and (+)-TA were made by weight using a five-place analytical balance (Model AG 245, Mettler-Toledo Inc., Switzerland) over the range of composition. Samples were weighed directly into glass vials (14 mm diameter  $\times$  45 mm length) and weights were kept consistent for each set of samples at  $\sim$ 500 mg. Samples were prepared over two ranges of composition (0 to 25% and 0 to 7%) consisting of ( $\pm$ )-TA as the minor component in the presence of (+)-TA.

#### NIRS Data Collection and Analysis

NIR spectra of the powder samples contained in glass vials were collected directly through the bottom of glass vials using a Foss NIRSystems Model 5000 monochromator equipped with a Rapid Content Sampler (Foss NIRSystems, Silver Springs, MD) over the wavelength region of

1100 to 2500 nm. Each spectrum was collected using 32 co-added scans. Three or ten spectra were collected and subsequently averaged for each sample. The samples were mixed between collection of each spectrum for  $\sim$ 60 seconds using a vortex mixer (Barnstead/ThermoLyne, Dubuque, IA). Previous studies have shown this procedure results in adequate mixing for binary mixtures.<sup>14</sup> Spectra were analyzed using Vision software (Version 2.11, Foss NIRSystems, Silver Springs, MD).

For data analysis, the second derivative of the response,  $\log(1/R')$  (where  $R'$  is the ratio of the reflected intensity of the sample to that of a nominally absorbing ceramic reference plate) vs wavelength was calculated using a progressive second order finite difference method with a segment size of 10 and gap size of 0. The second derivative value at a single wavelength was normalized using the second derivative value at a second wavelength (univariate method). Calibration plots were constructed using an inverted least squares regression method where the constituent value,  $c$ , is a linear function of the response,  $R_i$ , at some wavelength,  $\lambda_i$ , so that, Equation 1

$$c = K(0) + K(1)\bar{n}R_i \quad (1)$$

NIRS predicted compositions were calculated for each theoretical value and plotted against the theoretical composition using the univariate method. Analytical wavelengths were evaluated on the basis of achievement of high correlation coefficient, sensitivity, and validation as well as inspection and interpretation of the spectra. The denominator (or normalizing) wavelength was chosen by the software, but constrained to  $\pm$  300 nm of the analytical wavelength for most of the systems studied. Various calibration models were evaluated and those chosen were selected on the basis of the best coefficients of determination ( $R^2$ ) and standard errors of calibration (SEC).

#### Limit of Detection (LOD) and Limit of Quantification (LOQ)

The magnitude of the analytical background response was measured by analyzing a blank sample (0% analyte in the presence of other crystal form) ten times with mixing in between and calculating the standard deviation of the predicted composition. Three spectra were collected and subsequently averaged for each of the ten runs. The predicted composition was calculated using the univariate model. The standard deviation of the blank response multiplied by a factor, either 3 or 10, provides an estimate of the LOD and the LOQ, respectively. These theoretical limits were validated by the analysis of a

suitable number of samples prepared at compositions near these values.<sup>16</sup>

#### Instrument Error and Method Error

Studies were conducted to evaluate the primary sources of error inherent to the NIRS method. Variations in the radiation source and the detector response might contribute to instrument error and it was determined by assaying one sample 10 times without perturbation. Method error was assessed in the same manner except the samples were re-mixed in between collection of spectra to effectively change the sample presentation to the instrument. The predicted composition was calculated for these studies by using the univariate calibration model. The percent relative standard deviation (%RSD) was calculated from the replicate measurements.

#### Robustness of the Calibration Models

To examine whether the calibration models developed were robust and not affected by slight variations in the spectra that were not due to changes in the composition of the crystal forms, additional validation sample sets were prepared from different lots of materials and analyzed using the previously developed calibration models. The standard errors of the prediction (SEP) obtained for the new validation sets were compared with the SEPs of the original validation sets and the SECs of the calibration models. This study was conducted using different lots of (±)-TA and (+)-TA.

#### XRPD Studies

(±)-TA and (+)-TA samples as prepared for the NIRS studies were used for XRPD analysis. An aluminum sample holder with a cavity (22 mm × 18 mm × 3 mm) was back-filled to reduce preferred crystal orientation was used for all samples.

A Siemens Model D5000 X-ray diffractometer (40 kV, 30 mA, Bruker AXS Inc, Madison, WI) with a Kevex silicon-lithium energy sensitive detector (KevexSpectrace Inc, Sunnyvale, CA) was used for XRPD analysis. Data analysis was performed using Diffra<sup>plus</sup> Eva (Version 2.2, through Bruker AXS Inc, Madison, WI) software. Qualitative studies were performed over the range of 5 to 60° 2θ with a step size of 0.02° at a rate of 0.6° 2θ/min.

## RESULTS AND DISCUSSION

#### X-ray Powder Diffraction

(±)-TA and (+)-TA have distinctly unique XRPD patterns (Figure 1). The powder patterns were matched to those reported in the ICDD database ((±)-TA File # 31-1912, (+)

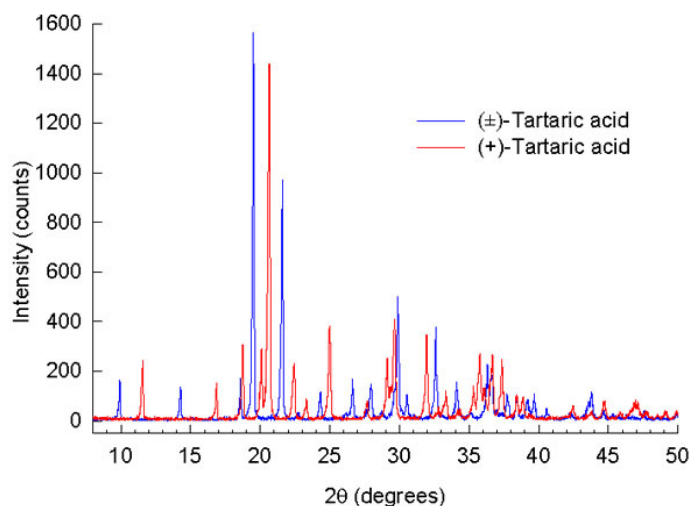


**Figure 1.** Experimental XRPD patterns of (±)-TA and (+)-TA.

–TA File # 31-1911).<sup>17</sup> The experimental XRPD patterns did not contain any additional peaks other than those observed in the ICDD reference patterns, verifying the identity of the crystal forms. The XRPD patterns of the unground powders were compared with their ground counterparts. Peak broadening was not observed in the ground samples as compared with the unground samples and therefore it was concluded that grinding had no observable effect on the crystallinity of (±)-TA and (+)-TA.

#### NIR Spectra

The NIR spectra of (±)-TA and (+)-TA exhibit the overtones and combinations corresponding to the fundamental bands originating in the mid-infrared region (Figure 2). As is common practice, a second derivative transformation was applied to resolve overlapping peaks due to multiple overtones and combinations and normalize the baseline shifts<sup>18</sup> (Figure 3). (±)-TA and (+)-TA have unique NIR spectra and several distinctive bands are seen in the regions of 1480 and 1520 nm (alcoholic O-H stretch), 1720 and 1760 nm (acidic O-H stretch), 1940 nm (C=O stretch), and 2040–2200 nm (O-H / C-O stretch combination) (Figure 2 and 3). The calculated first overtone region of alcoholic O-H stretch occurs in the region 1471 to 1617 nm. Two strong bands were observed for both (±)-TA and (+)-TA and the bands for (±)-TA at 1480 and 1520 nm were more intense than (+)-TA bands. Increased or stronger hydrogen bonding results in band shifts to higher wavelengths (lower frequencies) and vice versa. Because overtone and combination bands occur as the result of multiples of fundamental vibrations, frequency shifts related to hydrogen bonding have a greater effect on the overtone and combination bands than on their corresponding fundamentals.<sup>19</sup> Comparison of crystal structures of (±)-TA and (+)-TA shows that both forms have

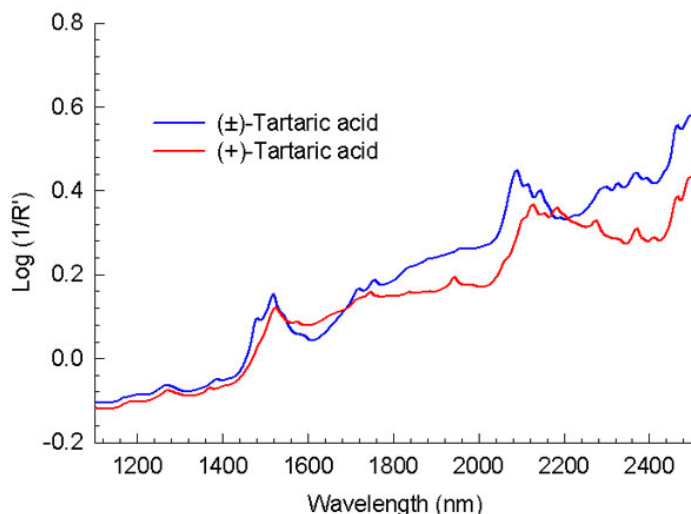


**Figure 2.** NIR spectra of (±)-TA and (+)-TA.

different molecular arrangements in their unit cells.<sup>20</sup> As a result, the hydrogen bonds patterns present in each form are different. (±)-TA forms dimers through the carboxylic groups whereas in (+)-TA, the acidic hydrogen is associated with a carbonyl on an adjacent molecule and the carbonyl oxygen is hydrogen bonded to an  $\alpha$ -hydroxyl of another molecule. The consequences of these differences are clearly manifest in their respective IR, Raman, and <sup>13</sup>C CP-MAS NMR spectra.<sup>21,22</sup> The impact on the NIR spectra (seen more clearly in the 2<sup>nd</sup> derivative plot, Figure 3) is that there is a distinctive up-shifting of peaks along with pronounced intensity differences.

## Quantification by NIR

### Wavelength Selection

In the quantitative model, the ratio of the second derivative response at two wavelengths reduces the effect of path-length differences caused by variations in particle size and packing.<sup>23</sup> Ideally, it should be possible to develop

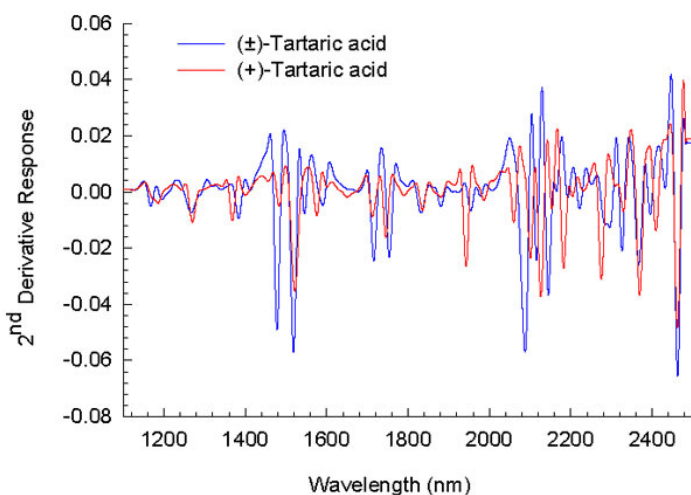


**Figure 3.** NIR second derivative spectra of (±)-TA and (+)-TA.

univariate calibrations using any of these wavelengths. However, we were interested in quantifying small amounts of the racemic compound in the presence of the pure enantiomer (0 to 25% and 0 to 7% composition range). When one form is present as a minor component, the change in the spectra as a function of composition is small at most wavelengths (Figure 4) compared with that seen with the two pure forms (Figure 3). Because the band at 1480 nm showed the greatest difference in the second derivative response with respect to racemic compound composition for the composition ranges evaluated, it was used to develop the univariate calibration models.

### Calibration and Validation

Calibration plots were constructed using the univariate method and two calibration models were developed using the ratio of second derivative response at 1480/1280 nm and 1480/1220 nm wavelengths for the 0 to 25% and 0 to 7% composition ranges, respectively (Figure 5). The regression statistics (coefficient of determination,  $R^2$ , and standard error of calibration, SEC) for the 1480/1280 nm and 1480/1220 nm models were comparable. Both of these calibration models provided high  $R^2$  values and low SECs (as % racemic compound composition). The 1480/1280 nm model was also used for the 0 to 7% composition range and it provided comparable results to the previously used model (Table 1). Independent validation sample sets were prepared over both composition ranges (0 to 25% and 0 to 7%) and used to test the predictive ability of the calibration models (Figure 5). Low absolute errors were obtained from validation of both calibration models (Table 2). The SEC

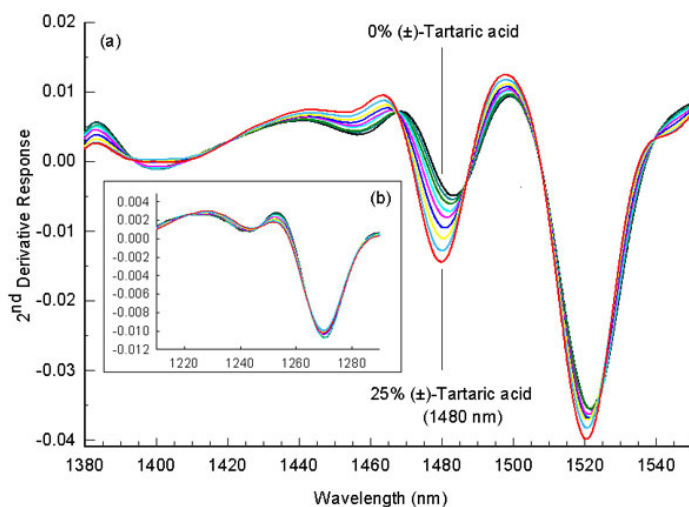


**Figure 4.** (a) NIR second derivative spectra of 0 to 25% (±)-TA in (+)-TA from 1380 to 1540 nm. Each spectrum represents increasing percent (±)-TA in (+)-TA from top to bottom at the indicated wavelength (1480 nm). The inset (b) shows the response in the wavelength region where the denominator wavelengths were chosen.

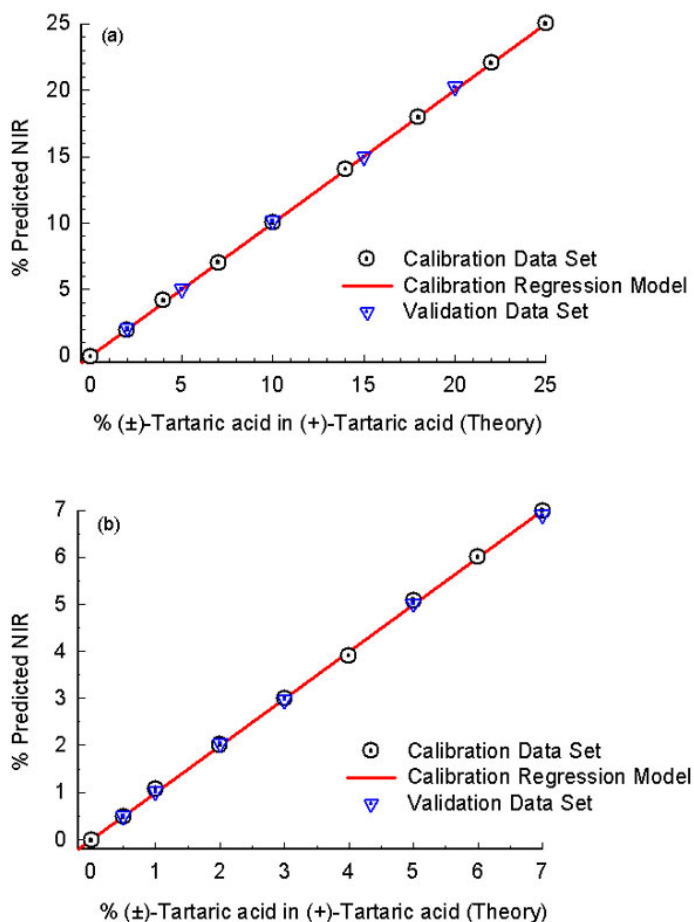


**Figure 5.** Calibration and validation plots of percent theoretical vs percent predicted by NIRS for (±)-TA in (+)-TA: a) for 0 to 25% composition range ( $R^2=0.9999$ ,  $SEC=0.07$  at 1480/1280 nm); b) for 0 to 7% composition range ( $R^2=0.9995$ ,  $SEC=0.06$  at 1480/1220 nm). Solid lines represent the linear regression calibration models.

and the SEP were used as estimators of the accuracy of NIR methods.<sup>23</sup> The SEC statistic is a measure of the deviation between the actual and predicted values for samples within the calibration set and the SEP is analogous except that it is applied to the samples within the validation set.<sup>24</sup> The SEPs were relatively low and comparable to the corresponding SECs (Table 1) and close correspondence of the SEC and SEP (as % racemic compound composition)

indicated good predictive ability of the calibration model. Considering the low range of composition studied, these results demonstrate that the NIR method has potential for high sensitivity as a solid-state method for quantifying the racemic compound content.

#### Robustness of the Calibration Models

Sometimes the NIR spectra of crystalline powders show differences in the spectra that are not attributable to changes in the crystal form, but due to variations in particle size and morphology, or the presence of residual solvent in the crystal forms. The second derivative processing may not completely normalize for these spectral differences. Therefore, to test whether the calibration model was affected by small variations in the physical characteristics of the crystal forms, additional validation sets for both composition ranges were prepared using different lots of (±)-TA and (+)-TA (obtained from a different vendor) to test the robustness of the original calibration models. These new validation samples were analyzed using the previously developed calibration models (Table 3). Slightly higher absolute errors were obtained for both composition ranges compared with the original validation results (Table 2). The SEPs from these validation sets were compared with the calibration SECs and the SEPs of the original validation sets (Table 1). The 2<sup>nd</sup> validation set SEPs had higher values than the original validation set (as well as calibration SECs) for both composition ranges, but were still within acceptable limits. The SEP for 0 to 25% validation set was significantly higher than the 0 to 7% validation set SEP for the 2<sup>nd</sup> validation set. Systematic trends were observed in estimation of the 2<sup>nd</sup> validation set samples for both composition ranges (Table 3). For the 0 to 25% range, predicted values exhibited a trend of decreasing negative absolute errors for the first three samples and increasing positive absolute errors for the remaining three samples. For the 0 to 7% range, the predicted values were higher than the actual values for all the validation samples. The systematic error might be inherent in the calibration models due to bias or slope effects. This was expected because the calibration and validation (new) samples were prepared

**Table 1.** Regression statistics for binary mixtures of (±)-TA and (+)-TA

Composition Range (±)-TA in (+)-TA	0 to 25%	0 to 7%	0 to 7%
Calibration Model	1480/1280 nm	1480/1220 nm	1480/1280 nm
Coefficient of Determination, $R^2$	0.9999	0.9995	0.9992
SEC*	0.07	0.06	0.07
Original Validation Set SEP <sup>†</sup>	0.11	0.05	0.07
2 <sup>nd</sup> Validation Set SEP (Using different lots of (±)-TA and (+)-TA than the calibration model)	0.36	0.14	0.26

\* Standard Error of the Calibration (as % (±)-TA composition)

† Standard Error of the Prediction (as % (±)-TA composition)

**Table 2.** Validation results for binary mixtures of ( $\pm$ )-TA in (+)-TA

0 to 25% ( $\pm$ )-TA in (+)-TA*			0 to 7% ( $\pm$ )-TA in (+)-TA†		
Actual %	Predicted	Absolute Error	Actual %	Predicted	Absolute Error
2.0	2.04	0.04	0.5	0.50	0.00
5.0	5.03	0.03	1.0	1.02	0.02
10.0	10.14	0.14	2.0	2.04	0.04
15.0	14.97	-0.03	3.0	2.97	-0.03
20.0	20.22	0.22	5.0	5.01	0.01
25.0	25.07	0.07	7.0	6.89	-0.11

\*1480/1280 nm calibration model used for this sample set.

†1480/1220 nm calibration model used for this sample set.

from different lots of ( $\pm$ )-TA and (+)-TA. However, if samples from both lots were included in the calibration sets and the number of samples were increased then it would result in reduction of the systematic error observed in the prediction of the new validation samples by the first calibration models. These results indicate that it is important to consider aspects of lot variation in building calibration models or to ensure that samples analyzed are composed from the same lots used in developing the calibration model for the most accurate results.

#### LOD and LOQ

LOD and LOQ for ( $\pm$ )-TA (in the presence of (+)-TA) were calculated using the 1480/1280 nm calibration model for the 0 to 25% composition range. The calculated LOD and LOQ values were 0.14% and 0.47%, respectively. Validation samples were prepared at 0.25%, 0.5%, and 1.0% and subsequently analyzed to verify the estimated LOQ. The results show that the model predicted well for 0.5% and 1.0% samples with low absolute errors and % RSDs (Table 4). The 0.25% sample had a significantly higher standard deviation and %RSD than the higher percentage samples. It can be concluded from these results that the practical LOQ lies between 0.25% and 0.5% on the basis of the 0 to 25% calibration range (1480/1280 nm) for the binary system. Additionally, LOD and LOQ for ( $\pm$ )-TA

were calculated the using 1480/1220 nm calibration model for the 0 to 7% composition range. The calculated LOD and LOQ values were 0.17% and 0.56%, respectively. The LOQ estimate was verified by again analyzing the 0.25%, 0.5%, and 1.0% ( $\pm$ )-TA samples. The results (Table 4) show that the practical LOQ is between 0.25% and 0.5% on the basis of the %RSDs of the samples. However, the absolute errors were significantly higher than those determined using the 0%-25% calibration model. The practically determined limits corresponded well with the calculated limits and demonstrate that NIRS can be used in this manner to assay small quantities of racemic compound in binary mixtures with reasonable accuracy and precision.

Additionally, the region of accurate quantification accessible by NIRS is comparable to other solid-state characterization methods for binary systems of this type. Elsabee and Pranker<sup>12</sup> reported a detection level of ~2% for mandelic acid using DSC. Stahly et al<sup>8</sup> using XRPD determined that the LOD and LOQ of (R,S)-ibuprofen in (S)-ibuprofen were 1% and 2%, respectively. Phadnis and Suryanarayanan<sup>7</sup> also analyzed (R,S)-ibuprofen in (S)-ibuprofen using a different XRPD methodology. They reported an LOD of ~3% and LOQ of 11%-13% with relative errors on individual samples of less than 10%. Hill et al<sup>11</sup> estimated that 5% optical or diastomeric impurity could be detected using Solid-State <sup>13</sup>C NMR. However,

**Table 3.** Validation results for binary mixtures of ( $\pm$ )-TA in (+)-TA using validation sample sets prepared from different lots of ( $\pm$ )-TA and (+)-TA

0 to 25% ( $\pm$ )-TA in (+)-TA*			0 to 7% ( $\pm$ )-TA in (+)-TA†		
Actual %	Predicted	Absolute Error	Actual %	Predicted	Absolute Error
2.0	1.66	-0.34	0.5	0.65	0.15
5.0	4.72	-0.28	1.0	1.18	0.18
10.0	9.76	-0.24	2.0	2.18	0.18
15.0	15.23	0.23	3.0	3.10	0.10
20.0	20.42	0.42	5.0	5.11	0.11
25.0	25.54	0.54	7.0	7.09	0.09

\*1480/1280 nm calibration model used for this sample set.

†1480/1220 nm calibration model used for this sample set.

**Table 4.** Instrument error, method error, and validation of LOQ for binary mixtures of (±)-TA and (+)-TA

Calibration Model	Actual % (±) -TA	0 to 25% (±)-TA in (+)-TA*			Actual % (±) -TA	0 to 7% (±)-TA in (+)-TA†		
		Mean Predicted <sup>  </sup>	Std Dev	% RSD		Mean Predicted <sup>  </sup>	Std Dev	% RSD
Instrument error	2.0	2.10	0.020	0.97	1.0	0.87	0.033	3.78
Method error	2.0	2.11	0.054	2.56	1.0	1.05	0.052	4.99
Validation of Limit of Quantification <sup>‡§</sup>	0.25	0.18	0.190	105.70	0.25	0.59	0.203	34.37
	0.50	0.49	0.035	7.09	0.50	0.94	0.058	6.21
	1.00	1.15	0.047	4.10	1.00	1.52	0.047	3.11

\*1480/1280 nm calibration model used for this sample set.

†1480/1220 nm calibration model used for this sample set.

‡Estimated LOD = 0.14%, LOQ = 0.47% using 1480/1280 nm model.

§Estimated LOD = 0.17%, LOQ = 0.56% using 1480/1220 nm model.

<sup>||</sup>n = 10

lower levels of detection would likely be obtained on modern equipment today because of improvements in NMR instrumentation. Calatozzolo et al,<sup>6</sup> using FTIR, reported a calibration SEP of <6% and achieved 17% RSD on a sample containing 2% (R,S)-dropropizine in (S)-dropropizine. On the basis of these relative comparisons among different compounds and methods, it can be concluded that NIRS compares favorably to other solid-state characterization methods for the application investigated and may represent a quantitative and timesaving advantage.

#### Instrument Error and Method Error

Instrument and method error studies were conducted to assess the potential primary sources of error inherent to the NIRS quantitative method. Instrument and method error were evaluated for the 0 to 25% and 0 to 7% calibration models using samples from the respective validation sets containing either 2% or 1% (±)-TA in (+)-TA. The %RSDs for instrument error were 1.0% and 3.8% for the 2% and 1% samples, respectively (Table 4). Comparison of the instrument error to the method error indicates the error introduced by mixing, sample orientation, and packing effects (Table 4). As expected, method errors were larger overall and ranged from ~2.5 to 5.0%. This indicated that variation due to sample presentation in the binary mixtures was the major contributor to the overall error. Additionally, the instrument and method error %RSD values were considerably lower for the 2% sample compared with the 1% sample results. A possible explanation for this may be that in the lower composition range mixing variation resulted in more error being incorporated in the calibration model relative to the 0%-25% composition range when the same number of samples. The error in the 0%-7% model could likely be reduced by increasing the number of calibration samples.

The instrument and method error studies indicate that it is reasonable to expect a minimum overall error (independent of sampling, day-to-day, and operator error) in the range of 2.5 to 5.0% for low level racemic compound quantification in binary systems using the sample-in-vial method and this detector configuration. The overall error is dependent on the composition range used, provided samples are in a suitable region of the calibration range and have sufficiently different spectra. Increased sensitivity, precision, and reduction of error in the NIRS method may be achieved by techniques that optimize sample presentation<sup>25</sup> and minimize additional sources of variability.<sup>26</sup>

#### CONCLUSIONS

NIRS was found to be a precise, accurate quantitative tool for determination of racemic compound level in binary powder mixtures of the enantiomeric crystal and its heterochiral form. Univariate calibration methods were developed for two composition ranges (0 to 25% and 0 to 7%) using a wavelength region that corresponded to an intrinsic variation in the two crystal forms attributable to differences in their crystalline structures. The validated LOQ demonstrated that NIRS could be used to quantify as low as 0.5% of racemic compound in the pure enantiomer with relatively low error (2.5 to 5.0%). A simple and rapid quantitative solid-state methodology previously applied to polymorph pairs, anhydrate-hydrate pairs and crystalline-amorphous form pairs has been shown to extend to a crystalline racemic compound and its corresponding enantiomorph.

#### ACKNOWLEDGMENTS

This work was conducted at The University of Iowa, College of Pharmacy, in partial fulfillment of the require-

ments for the Masters of Science Degree for Aditya D. Patel in the Graduate College

The authors acknowledge Dr. Z. Jane Li of Pfizer Inc (Groton, CT) for helpful suggestions and comments.

## REFERENCES

1. Millership JS, Fitzpatrick A. Commonly used chiral drugs: a survey. *Chirality*. 1993;5:573–576.
2. Drayer DE. Pharmacodynamic and pharmacokinetic differences between drug enantiomers in humans: overview. *Clin Pharmacol Ther*. 1986;40:125–133.
3. Jacques J, Collet A, Wilen SH. In: *Enantiomers, Racemates and Resolutions*. New York, NY: John Wiley & Sons, 1981.
4. Duddu SP, Grant DJ. Effects of configuration around the chiral carbon atoms on the crystal properties of ephedrinium and pseudoephedrinium salicylates. *Pharm Res*. 1994;11:1549–1556.
5. Piyarom S, Yonemochi E, Oguchi T, Yamamoto K. Effects of grinding and humidification on the transformation of conglomerate to racemic compound in optically active drugs. *J Pharm Pharmacol*. 1997;49:384–389.
6. Calatuzzolo M, Celentano G, Clerici F, Giammarusti G, Stradi R. FT-IR spectroscopy for the evaluation of the enantiomeric purity of levodropropizine: comparison with HPLC analysis. *Boll Chim Pharm*. 1993;132:467–471.
7. Phadnis NV, Suryanarayanan R. Simultaneous quantification of an enantiomer and the racemic compound of ibuprofen by X-ray powder diffractometry. *Pharm Res*. 1997;14:1176–1180.
8. Stahly GP, McKenzie AT, Andres MC, Russell CA, Johnson P. Determination of the optical purity of ibuprofen using X-ray powder diffraction. *J Pharm Sci*. 1997;86:970–971.
9. Jaroszewski JW, Olsson A. Determination of enantiomeric purity of nicotine in pharmaceutical preparations by  $^{13}\text{C}$ -NMR in the presence of chiral lanthanide shift reagent. *J Pharm Biomed Anal*. 1994;12:295–299.
10. Hanna GM. Determination of enantiomeric composition of ibuprofen in bulk drug by proton nuclear magnetic resonance spectroscopy with a chiral lanthanide chelate. *J Pharm Biomed Anal*. 1997;15:1805–1811.
11. Hill HDW, Zens AP, Jacobus J. Solid-state NMR spectroscopy, distinction of diastereomers and determination of optical purity. *J Am Chem Soc*. 1979;101:7090–7091.
12. Elsabee M, Pranker RJ. Solid-state properties of drugs. Part 3. Differential scanning calorimetry of chiral drug mixtures existing as racemic solid solutions, racemic mixtures or racemic compounds. *Int J Pharm*. 1992;86:221–230.
13. Buchanan BR, Ciurczak EW, Grunke AQ, Honigs DE. Determination of enantiomeric purity of valine via Near-infrared reflectance spectroscopy. *Spectroscopy*. 1988;3:54–56.
14. Luner PE, Majuru S, Seyer JJ, Kemper MS. Quantifying crystalline form composition in binary powder mixtures using near-infrared reflectance spectroscopy. *Pharm Dev Technol*. 2000;5:231–246.
15. Seyer JJ, Luner PE, Kemper MS. Application of diffuse reflectance near-infrared spectroscopy for determination of crystallinity. *J Pharm Sci*. 2000;89:1305–1316.
16. The United States Pharmacopeia. USP24. Rockville, MD: US Pharmacopeial Convention, 2000;2149–2152.
17. Powder Diffraction File. Swarthmore, PA: International Center for Diffraction Data, 1989.
18. Kirsch JD, Drennen JK. Near-infrared spectroscopy: applications in the analysis of tablets and solid pharmaceutical dosage forms. *Appl Spectrosc Rev*. 1995;30:139–174.
19. Workman JJ, Jr. Interpretive Spectroscopy for Near Infrared. *Appl Spectrosc Rev*. 1996;31:251–320.
20. Luner PE, Patel AD, Swenson DC. (+/-)-tartaric acid. *Acta Crystallogr C*. 2002;58:O333–O335.
21. Patel AD, Swenson DC, Luner PE. Solid-state characterization and crystal structure of dl-tartaric acid. *PharmSci*. 2000;2:3587.
22. Patel AD. In: Solid-state characterization and quantitative analysis of crystal forms using near infrared reflectance spectroscopy [master's thesis]. Iowa City, Iowa: University of Iowa, College of Pharmacy, 2000.
23. Honigs DE. Near infrared analysis. *Anal Instrum*. 1985;14:1–62.
24. Workman JJ, Burns DA, Ciurczak E, ed. NIR Calibration. In: *Practical Spectroscopy Series: Handbook of Near-Infrared Analysis*. 1st ed. New York: Marcel Dekker Inc, 1992;274–275.
25. Borer MW, Zhou X, Hays DM, Hofer JD, White KC. Evaluation of key sources of variability in the measurement of pharmaceutical drug products by near infrared reflectance spectroscopy. *J Pharm Biomed Anal*. 1998;17:641–650.
26. Yoon WL, Jee RD, Moffat AC. Optimisation of sample presentation for the near-infrared spectra of pharmaceutical excipients. *Analyst*. 1998;123:1029–1034.